Diffusion-weighted MRI: new paradigm for the diagnosis of interstitial oedematous pancreatitis

Massimo Tonolini[1], Salvatore Di Pietro[1,2]

[1]Department of Radiology, "Luigi Sacco" University Hospital, Milan, Italy; [2]Post-graduation School in Radiodiagnostics, University of Milan, Milan, Italy

Correspondence to: Massimo Tonolini, MD. Department of Radiology, "Luigi Sacco" University Hospital, Via G.B. Grassi 74, 20157 Milan, Italy. Email: mtonolini@sirm.org.

Introduction

Acute pancreatitis (AP) represents an acute, non-infectious inflammatory process affecting the pancreatic gland. The pathophysiology of AP involves an inappropriate activation of trypsinogen and other digestive and proteolytic enzymes, which causes damage to acinar cells and release of cytokines and vasoactive mediators, ultimately leading to oedema and apoptosis of pancreatic tissue. This condition has a wide range of clinical manifestations and potential complications, ranging from self-limiting events to life-threatening emergency with systemic manifestations and multiple organ failure. A recent review demonstrated an increasing incidence of AP (median 3.4% per annum) in Europe, with largely variable figures (from 4.6 to 100/100,000 people/year) among different countries. Specifically, the incidence is highest in eastern (mostly alcohol-related) and northern Europe, and lower (mostly gallstone-related) in southern European populations (1). Mortality is largely due to severe necrotizing forms but unrelated to age, and occurs in up to 7.8–21% of patients (2,3).

The diagnosis of AP relies on the presence of at least two of the following three features: (I) sudden onset of upper abdominal pain; (II) serum amylase and/or lipase levels greater than three times the upper limit of normal; and/or (III) consistent imaging findings. The severity of AP is stratified according to presence of organ failure, local complications (necrosis and fluid collections) and systemic complications (*Table 1*). Several clinical systems help predicting the severity of AP, such as the Ranson score, the Acute Physiology and Chronic Health Examination

(APACHE) II and the Bedside Index for Severity in AP. However, these clinical scores typically require 24–48 hours of observation to be assessed (4).

Current role of imaging in AP

Aiming to establish a standardized terminology, in 2012 the revised Atlanta classification divided AP into two distinct subtypes, namely interstitial oedematous pancreatitis (IEP) and necrotizing AP, respectively based on the absence or presence of necrosis in either the pancreatic parenchyma or peripancreatic tissues. Furthermore, in the Atlanta classification peripancreatic fluid collections are categorized according to time elapsed and type of AP. In IEP, acute peripancreatic fluid collections containing simple fluid may evolve into pseudocysts after 4 weeks. In necrotizing AP, acute necrotic collections contain variable amounts of debris and blood and may persist as walled-off necrosis. The development of necrosis indicates that the inflammatory cascade has evolved into the formation cellular apoptosis and loss of microvascular supply in the pancreatic gland, which explains the characteristic devascularisation of necrotic portions on computed tomography (CT) and magnetic resonance imaging (MRI). In the vast majority of patients, CT is the most widely used technique for confirming the diagnosis of AP and detecting possible complications, because it is widely available on a 24-hour basis, is rapidly obtained within minutes, and provides robust imaging even in critically ill patients. However, CT involves administration of non-negligible doses of ionizing radiation, and assessment of pancreatic necrosis requires

Table 1 Severity stratification of acute pancreatitis

Grade	Organ failure	Local and systemic complications	Mortality
Mild	Absent	Absent	Exceptional
Moderately severe	Transient (resolves within 48 hours)	Possible	Rare (2%)
Severe	Persistent (beyond 48 hours)	Present	20–30%

intravenous administration of iodinated contrast medium, which is potentially nephrotoxic in patients with impaired renal function (5-7).

In the setting of AP, CT has consistently shown clinical value in predicting disease severity and clinical outcome. Developed by Balthazar *et al.* in 1990, the CT severity index (CTSI) is the most widely used system used in both clinical and research settings, based on the assessment of the pancreatic parenchymal changes and the associated fluid collections. In the CTSI, the role of the radiologist lies in determining the presence and extent of necrosis, semi-quantified as <30%, 30–50% and >50%. Later in 2004, the modified CTSI (m-CTSI) simplified the assessment of extent of the pancreatic parenchyma and peripancreatic inflammation, while accounting for some limitations of the CTSI by incorporating extrapancreatic manifestations. Ultimately, the CTSI and the m-CTSI did not reveal significant differences in evaluating the severity of AP compared with the clinical APACHE II score, as both CT indices accurately diagnose disease severity and proved equivalent with regards to predicting the need for intervention (7,8).

In clinically mild IEP, routine CT is not warranted due to the transient nature of the disease and the frequent poor yield of imaging, as up to one-third of patients have no detectable CT abnormalities. The usual CT findings observed in IEP include peripancreatic inflammatory changes (fat stranding and/or fluid), diffuse or localized enlargement of the pancreas with preserved homogenous contrast enhancement of the viable oedematous parenchyma. The key finding that discriminates necrotizing AP from IEP is the loss of enhancement in all or part of the pancreas corresponding to necrotic areas. CT is routinely performed in patients with severe symptoms to exclude alternative causes of abdominal pain. However, in AP CT at time of admission is not better for predicting severity than clinical scoring indices and therefore should not be routinely performed if the diagnosis is established on the basis of consistent clinical and laboratory data. Furthermore,

radiologists are well aware that CT performed within 72 h from symptom onset may underestimate the severity of AP since in the early stages necrosis may not have adequate time to develop, and repeated CT scanning is required in patients without significant clinical improvement to reassess the presence and extent of pancreatic necrosis (5-7).

Finally, relying on CT to assess and monitor AP may require several full-dose CT studies (often with multiphasic protocols), thus leading to high cumulative radiation exposure in relatively young patients: this is particularly true for those with severe AP, despite the fact that some studies reported that CT findings rarely changed management (9-11).

Using MRI in AP

Therefore, using non-ionizing MRI instead of CT is appealing to limit the radiation exposure. Unfortunately, in the past MRI usage was limited not only by availability, but also by lengthy acquisitions including multiple breath-hold sequences in ill patients with poor cooperation. During the last decade, technical advancements such as the use of multichannel phased-array coils, parallel imaging, respiratory triggered and navigator-echo-based techniques allowed for faster, motion-resistant acquisitions with improved spatial resolution. MRI can accurately diagnose AP with higher soft-tissue contrast compared to CT. Similarly to CT, MRI can be used for the diagnosis and severity grading in AP: the proposed MR severity index (MRSI) significantly correlated with Ranson scores, CTSI, C-reactive protein levels, duration of hospitalization and clinical outcome. Furthermore, MRI including MR-cholangiopancreatography (MRCP) sequences comprehensively allows non-invasive assessment of coexistent cholelithiasis, pancreatic duct anatomy (such as underlying pancreas divisum) and integrity (disconnected pancreatic duct syndrome) (6,12).

Out-of-phase and fat-saturated T1-weighted images allow confident assessment of pancreatic gland size and

configuration. Compared to remaining pancreas AP, the involved pancreatic regions usually appear iso- to mildly hypointense on T1-weighted, iso- to mildly hyperintense on heavily T2-weighted images. Peripancreatic oedematous stranding and fluid are well perceptible on fat-saturated T2-weighted sequences. The AP-related enlargement of the pancreatic gland may be diffuse or localized and accompanied by homogeneous, normal enhancement on dynamic gadolinium-enhanced T1-weighted imaging. Conversely, the necrotic pancreatic tissue is inhomogeneous and does not enhance. Finally, MRI is superior to CT for detection of internal consistency and characterization of collections, by showing internal T2-hypointense necrotic debris that differentiates acute necrotic collections and walled-off necrosis from simple fluid pseudocysts (12,13).

Introducing diffusion-weighted MRI

Recently adopted in everyday radiological practice, diffusion-weighted imaging (DWI) is a relatively new MRI technique which holds great potential in abdominal imaging, in particular for detection and characterization of focal lesions and for assessment of diffuse parenchymal diseases. DWI is appealing because it is obtained within a few minutes and does not require gadolinium contrast administration. DWI depicts molecular diffusion, a physical process which reflects the Brownian motion of water protons within living biologic tissues, and provides functional information concerning tissue cellularity and the status of cell membranes. Specifically, tissues with low cellularity or consisting of cells with disrupted membranes allow greater movements of water molecules. Conversely, restricted (impeded) diffusion may be secondary to tumour, cytotoxic oedema or abscess. The sensitivity of DWI sequences is adjusted by varying the b coefficient, a value which refers to the strength of the diffusion sensitizing gradient and is measured in seconds per square millimeter (s/mm^2). The apparent diffusion coefficient (ADC) is a quantitative parameter which reflects the combined effects of water diffusion in the extracellular extravascular space and perfusion in the capillary network. Calculated during post processing from DWI acquisitions, the ADC value is displayed as a parametric map from which ADC values of different tissues can be derived by placing regions-of-interest (ROI). For instance, DWI has excellent sensitivity for malignant lesions since increased cellularity is associated with decreased diffusion and therefore shows up as visually hyperintense on high b value DWIs, with corresponding low ADC values compared to spared areas. Non-neoplastic lesions may show diffusion restriction due to inflammation, presence of pus or high cellularity. Currently, most evidence concerns characterization of pancreatic masses rather than diffuse processes such as AP. Recommendations for DWI of the pancreas include use of at least 4 b values (0, 150, 400–500 and 800–1,000) (14,15).

Some recent studies revealed that the AP-involved pancreatic parenchyma shows restricted diffusion compared to healthy pancreas. The underlying mechanism involves a combination of acinar cell death, leukocytes invading acinar spaces, deposition of fibrin in the intercellular space and microthrombi in blood vessels (16).

In 2009, Shinya et al. first reported the DWI signal intensity changes in AP, suggesting an improved diagnosis of AP with MRI including DWI over non-contrast CT (13,17). Later in 2012, Thomas et al. confirmed increased DWI signal intensity and decreased ADC in patients with AP compared with those with a normal pancreas, suggesting a cut-off value of 1.62×10^{-3} mm^2/s (using b 800 s/mm^2) with 93% sensitivity and 87% specificity for diagnosing AP, and reporting the potential reversal of diffusion restriction after clinical normalisation (18). Yencilek et al. reported progressively lower ADC values as the severity of the AP increased according to the Balthazar classification, and confirmed the ability of DWI to detect AP even in Balthazar grade A cases without abnormal findings on CT. The mean pancreatic ADC values in AP [$(1.19 \pm 0.32) \times 10^{-3}$ mm^2/s] was significantly lower than in the normal group [$(1.78 \pm 0.29) \times 10^{-3}$ mm^2/s] (P<0.001). In the subgroup analysis, ADC values in each group were significantly lower than in the control group. In addition, lower ADC values were noted along with increasing severity of AP according to the Balthazar classification (19).

Therefore, the ability of DWI to depict the acutely inflamed pancreatic tissue without use of contrast medium is particularly beneficial in mild forms of AP. Another more recent study confirmed the added value of DWI in identification of mild IEP with Ranson scores up to 3, in which the mean ADC were significantly lower [$(1.46 \pm 2.80) \times 10^{-3}$ mm^2/s] compared to healthy subjects [$(1.69 \pm 2.26) \times 10^{-3}$ mm^2/s] (20).

The key limitation of DWI is the lack of standardization. Unfortunately, the ADC values of healthy pancreas significantly vary among different manufacturers and scanners, acquisition protocols and parameters. Furthermore, reported ADC values show high standard deviation (SD), attributable to a combination of factors,

Table 2 Acquisition protocol for non-contrast MRI of the upper abdomen in patients with suspected acute diseases of the biliopancreatic tract on 1.5 Tesla scanner (Ingenia, Philips, The Netherlands) with 16-channel phased-array coils and parallel imaging (SENSE technology)

Sequence (after 3-plane localizer)	Scan plane	TR (msec)	TE (msec)	Slice thickness (mm)	Gap (mm)	Matrix	NEX	Duration (min:sec)
SSH T2-weighted	Coronal	6,500	90	4–5	0.5	272×238	2	0:26
SSH T2-weighted	Axial	7,900	80	5	0.5	288×217	2	0:32
Fat suppressed SSH T2-weighted	Axial	6,498	80	4	0.4	220×167	2	0:26
EPI Diffusion-weighted (b values 0, 50, 600, 800)	Axial	N/A	N/A	6	0.6	132×114	6	4:18
In-phase T1-weighted	Axial	10	4.6	6	0.6	236×154	1	1:45
Out-phase T1-weighted	Axial	10	2.3	6	0.6	236×154	1	1:45
Breath-hold m-DIXON T1-weighted (*alternative to in- & out-phase T1-weighted*)	Axial	Shortest	1.8–4 (flip angle 15°)	6	−0.6	308×202	1	0:23
Thick slab MRCP	Oblique-coronal	8,000	800	40	−0.9	260×260	1	4:06
Radial volumetric (3D) MRCP	Oblique-coronal	N/A	600	1.8	1	300×239	1	1:12

SSH, single shot spin-echo; EPI, echo planar imaging; NEX, number of excitations; TR, repetition time; TE, echo time; N/A, not available.

including heterogeneous distribution of inflammation within the pancreas, and interobserver variation secondary to difficulties in placing ROIs in non-enlarged glands. Therefore, the use of normalization (ratio of lesion ADC to ADC of normal parenchyma) has been suggested to compare results among different studies (14).

Personal experience

Materials and methods

From early 2017 to August 2018, we collected all patients hospitalized from our ED with a clinical and laboratory diagnosis of AP. Among these, we selected those who had both urgent CT and MRI at our Center within a week, and excluded those with imaging evidence of pancreatic necrosis. The resulting cohort of 16 patients included 11 males (68.7%) and 5 women (31.3%) with a mean age of 59.8 years (range 22 to 88 years). The majority (10/16, 62.5%) had gallstone-related AP and four of them had history of previous cholecystectomy. Underlying pancreas divisum was detected in a patient. At admission, the mean white blood cell (WBC) count was 14,457 cells/mmc (range 7,050 to 22,310 cells/mmc), mean C-reactive protein was 60 mg/L (range 2 to 160 mg/L); mean lipase level was 2,996 U/L (range 13 to 13,780 U/L).

All patients underwent unenhanced and contrast-enhanced CT on a 64-slice multidetector Brilliance 64-slice CT scanner and non-contrast MRI on our 1.5 Tesla Ingenia MRI (both from Philips, The Netherlands) using a 16-channel phased array coil and parallel imaging (SENSE technology). Our rapid (scan time not exceeding 15 minutes after patient positioning, including scout views) non-contrast MRI acquisition protocol of the upper abdomen for patients with suspected acute biliopancreatic diseases is listed in *Table 2*. At the radiologist's discretion, when pancreatic necrosis is suspected, examination may be completed with optional dynamic MRI acquisition after intravenous injection of 0.1 mL/kg of 1-molar gadobutrol (Gadovist; Bayer Schering, Berlin, Germany) at an infusion rate of 2 mL/s through a power injector followed by 20 mL of normal saline bolus, using a bolus triggering technique and THRIVE (T1W high resolution isotropic volume examination) sequences, including late arterial (pancreatic), portal venous and full venous phases.

During post-processing, ADC maps were visualized in comparison with conventional T2-weighted and DWI images, and ADC values and SD were measured at four pancreatic regions (head, isthmus, body and tail) and on iliopsoas muscles by placing region-of-interests (ROI) with an approximate size of 10 mm^2. To avoid spurious results,

Table 3 Apparent diffusion coefficient (ADC) values of the pancreas in patients with interstitial oedematous acute pancreatitis

Pancreatic region	Mean ADC (×10^{-3} mm^2/s)	ADC standard deviation (×10^{-3} mm^2/s)	ADC range
Head	1.32	0.13	0.73–1.99
Isthmus	1.27	0.15	0.77–1.92
Body	1.32	0.12	0.63–1.96
Tail	1.35	0.15	0.89–2.27
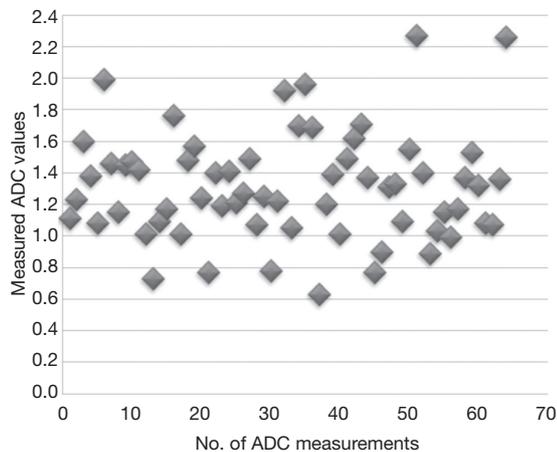
Figure 1 Distribution of measured apparent diffusion coefficient (ADC) values (along Y axis, ×10^{-3} mm^2/s) of four pancreatic regions in 16 patients with interstitial oedematous pancreatitis (IEP).

Figure 2 Distribution of ADC values (along Y axis, ×10^{-3} mm^2/s) of four pancreatic regions in 16 patients with IEP, normalized using the ADC value of the iliopsoas muscle in the same patient. ADC, apparent diffusion coefficient; IEP, interstitial oedematous pancreatitis.

measures were repeated and mean figures were calculated.

Furthermore, to provide a basis for comparison with MRI obtained on different scanners, normalized ADC values were calculated for each pancreatic region by dividing the measured ADC by the mean ADC value of the iliopsoas muscle in the same patient.

Results

Table 3 and *Figure 1* respectively present a summary and the graphical distribution of the resulting ADC measurements. The 14.5% of ADC measurements above 1.6×10^{-3} mm^2/s mostly represent regions of spared parenchyma. Using the same protocol, ADC values in a cohort of patients without clinical and laboratory evidence of liver, biliary and pancreatic diseases measure 1.8×10^{-3} mm^2/s on average.

The normalized ADC values are shown graphically in *Figure 2*. Compared to the lowest native ADC values, a similar percentage of normalized ADC measurements exceeded 1.1×10^{-3} mm^2/s.

Conclusions

Practical approach

DWI is highly sensitive to the presence of IEP and therefore allows differentiation from other diseases with a similar clinical presentation. From our experience, when discussing with clinicians and emergency physicians we increasingly recommend a rapid noncontrast MRI including high b value DWI (such as the protocol proposed in *Table 2*) as a valid non-invasive option to diagnose mild AP. In particular MRI is preferable to contrast-enhanced CT in young people in which obviating radiation use is recommended, and in patients with impaired renal function or allergy to iodinated contrast medium. CT may remain the first examination in elderly and uncooperative patients, to provide a rapid differential diagnosis when alternative causes of acute abdomen are being considered, and in clinically severe AP forms to promptly diagnose necrosis and collections (21).

In everyday practice, after MRI acquisition at our
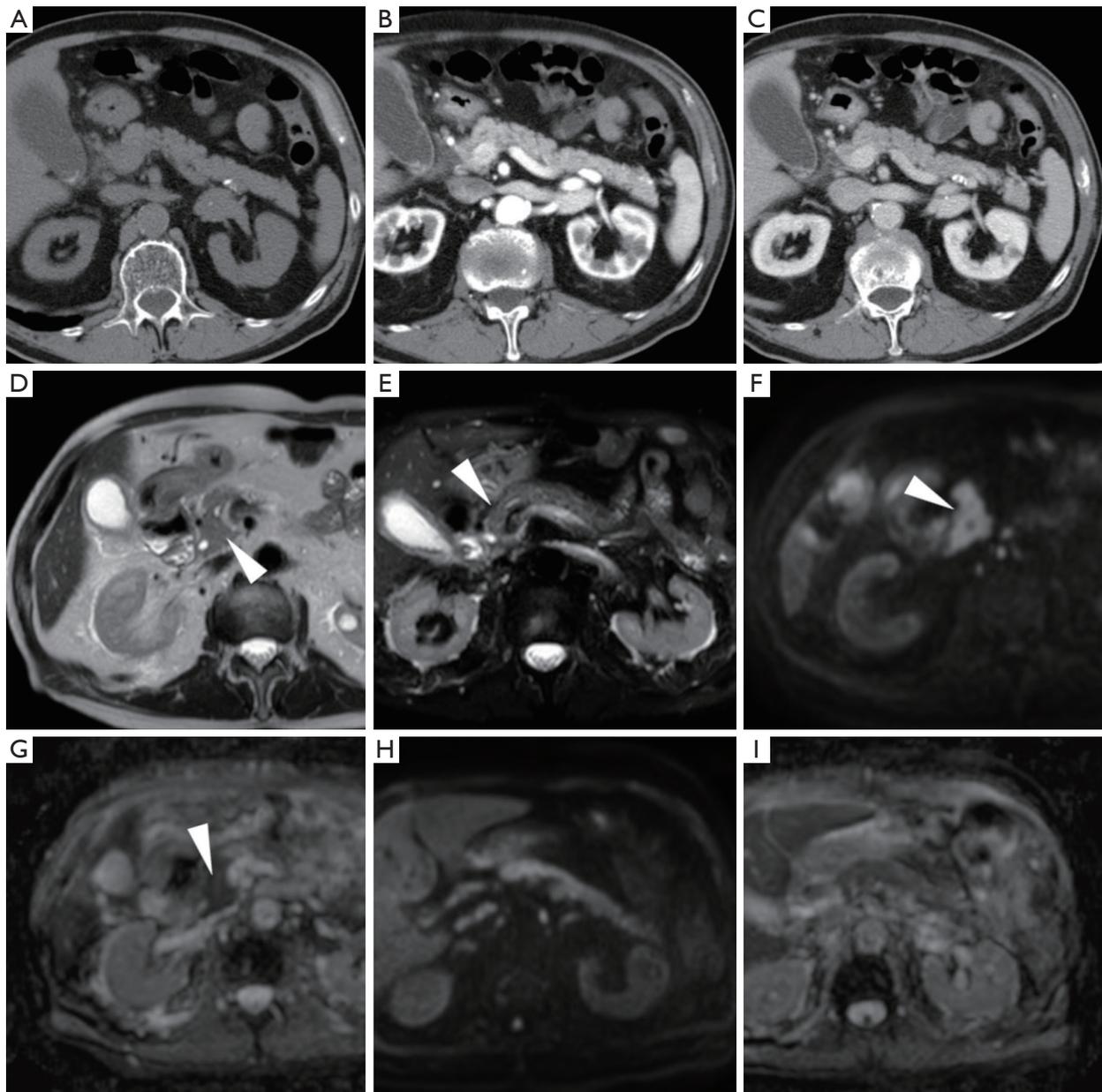
Figure 3 In an 84-year-old male with gallstone-related IEP multidetector CT including precontrast (A), enhanced pancreatic (B) and portal venous (C) CT acquisitions showed near-normal findings concerning pancreatic size, enhancement and surrounding planes. Alternative causes of upper abdominal pain were excluded. Further investigation with MRI confirmed normal size, morphology and signal intensity of the pancreatic head and isthmus (arrowheads) on T2-weighted (D,E with fat suppression) images, and revealed visual hyperintensity on diffusion-weighted imaging (DWI, F,H) and corresponding low signal on apparent diffusion coefficient (ADC) maps (G and I, mean measured value 1.01×10^{-3} mm^2/s). The altered DWI decreased along the pancreatic body and normalized at the tail. IEP, interstitial oedematous pancreatitis.

Institution we suggest findings consistent with clinical and laboratory diagnosis of IEP when visual analysis shows clear hyperintensity of regions or the entire pancreas.

Figures 3-5 show three patients from our series as examples of how DWI diagnoses IEP in patients with no or limited CT findings. Furthermore, we usually place three or four
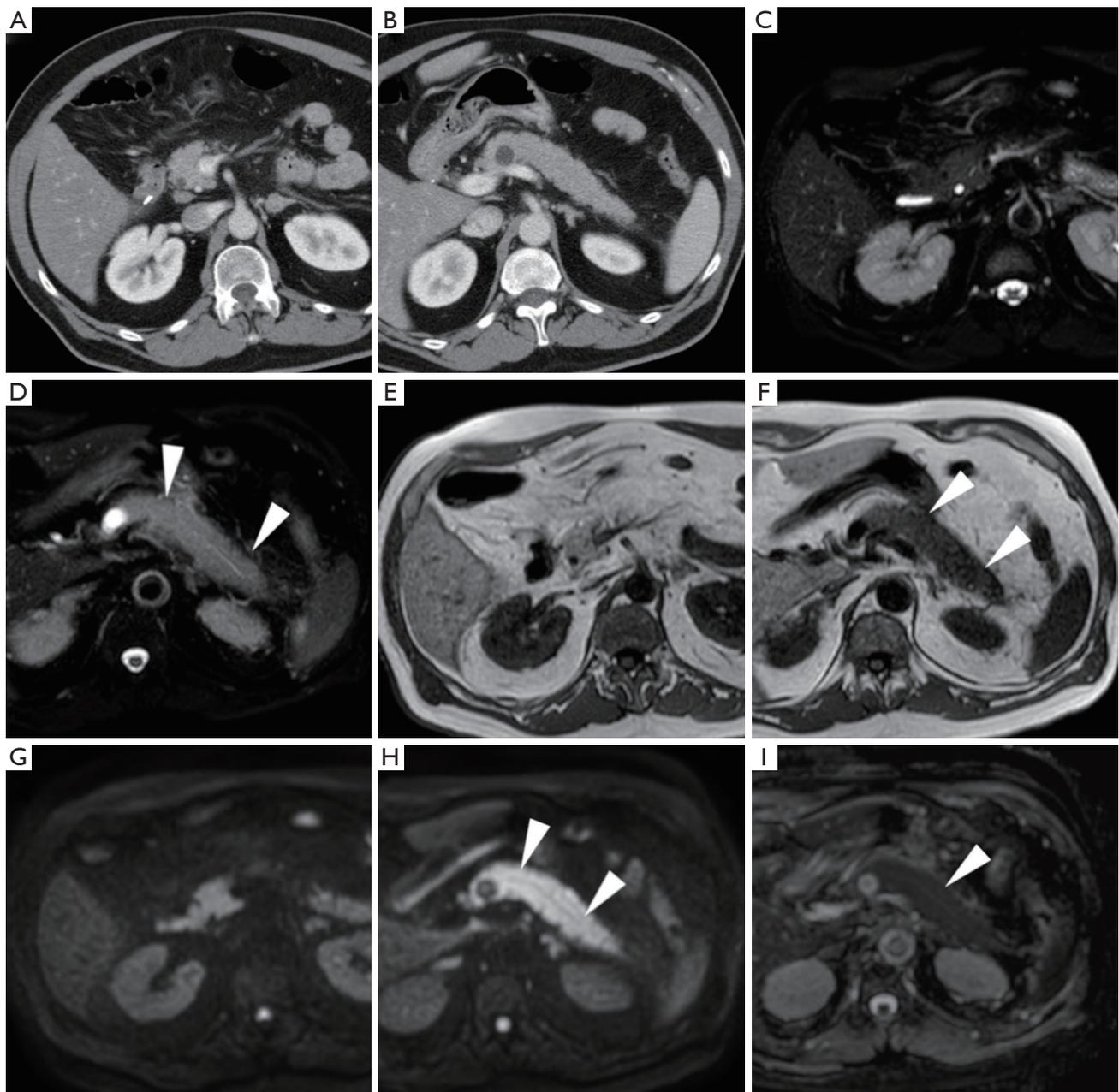
Figure 4 In a 62-year-old male with IEP and history of cholecystectomy, contrast-enhanced CT (A,B) did not reveal any abnormality. At MRI, compared to the normal pancreatic head, the body and tail (arrowheads) showed moderate uniform thickening, increased signal intensity on fat-saturated T2-weighted images (C,D) and hypointensity on T1-weighted images (E,F) reflecting oedema, and strong hyperintensity on DWI (G,H) with corresponding low ADC (I, mean 0.70×10^{-3} mm^2/s). IEP, interstitial oedematous pancreatitis; ADC, apparent diffusion coefficient; DWI, diffusion-weighted imaging.

ROIs along the pancreatic parenchyma to obtain ADC measurements, and confirm restricted diffusion when ADC values measure below 1.6×10^{-3} mm^2/s. On other scanners, 1.1×10^{-3} mm^2/s may be proposed as a cut-off for confirming restricted diffusion in high b value DWI acquisitions obtained with different sequence parameters.

gs.amegroups.com   *Gland Surg* 2019;8(2):197-206
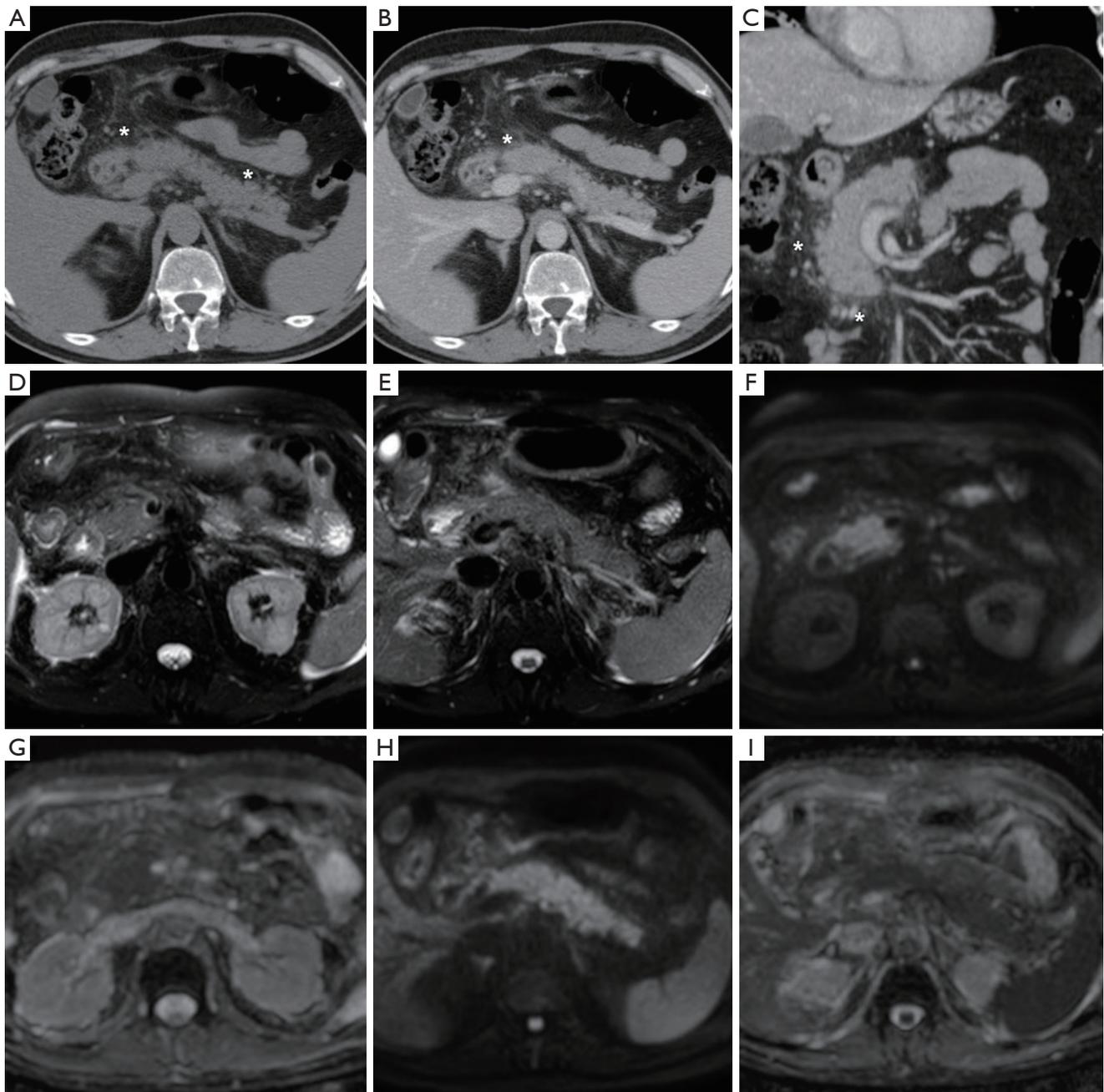
Figure 5 A 44-year-old male with gallstone-related IEP had CT (A,B,C) findings of peripancreatic fat stranding (*), preserved pancreatic size and enhancement. At MRI, fat-suppressed T2-weighted images (D,E) better showed thin fluid effusion along periduodenal planes and retroperitoneal fasciae. Pancreatic diffusion was homogeneously restricted along the entire gland (F,H) with corresponding low ADC signal (G,I). IEP, interstitial oedematous pancreatitis; ADC, apparent diffusion coefficient.

Tips for differential diagnosis

The major limitation of DWI in the pancreas remains its inability to reliably differentiate between mass-forming AP and tumours, particularly ductal adenocarcinoma, because of the overlapping ADC values. Therefore, DWI should not be interpreted in isolation but together with physical and laboratory findings, conventional MRI sequences, MRCP
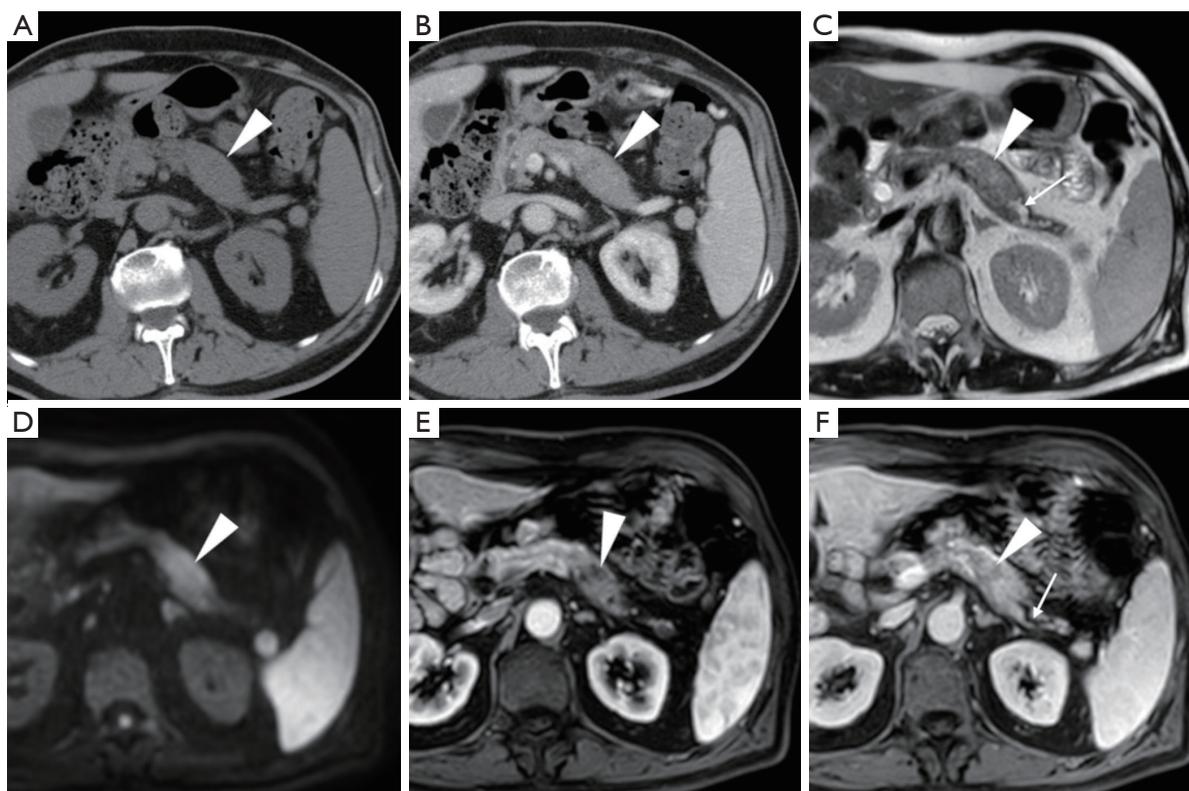
Figure 6 Differential diagnosis with pancreatic carcinoma. In a 58-year-old male with unspecific upper abdominal pain (not included in the personal series) precontrast (A) and enhanced (B) CT images showed fusiform enlargement with smooth margins of the pancreatic tail (arrowheads). At MRI, the lesion (arrowheads) showed moderately increased and inhomogeneous T2-weighted signal (C), restricted diffusion (D), poor inhomogeneous enhancement on pancreatic (E) and portal venous (F) phases of dynamic gadolinium-enhanced acquisition. Additionally, upstream dilatation of the obstructed main pancreatic duct (thin arrows in C,F) reinforced the suspicion of tumour, which was ultimately confirmed at endoscopic ultrasound guided biopsy.

and contrast-enhanced study. Specifically, young patient age and clinical data consistent with an acute presentation favour AP over cancer. Conversely, an insidious history should suggest the presence of a malignancy. From the imaging perspective, focal AP manifesting as hypoenhancing mass is easily misinterpreted as tumour. Radiologists should consider additional findings such as peripancreatic oedema, effusion and collections that may strengthen a diagnosis of AP. On the other hand, signs of infiltration of adjacent structures and obstruction of the main pancreatic duct favour the possibility of cancer (*Figure 6*). Strict imaging follow-up and further investigation with endoscopic ultrasound-guided biopsy are warranted in questionable cases (14,22,23).

Acknowledgements

None.

Footnote

References

1. Roberts SE, Morrison-Rees S, John A, et al. The incidence and aetiology of acute pancreatitis across Europe. Pancreatology 2017;17:155-65.
2. Gullo L, Migliori M, Olah A, et al. Acute pancreatitis in five European countries: etiology and mortality. Pancreas 2002;24:223-7.
3. Popa CC, Badiu DC, Rusu OC, et al. Mortality prognostic factors in acute pancreatitis. J Med Life 2016;9:413-8.
4. Pezzilli R, Zerbi A, Di Carlo V, et al. Practical guidelines for acute pancreatitis. Pancreatology 2010;10:523-35.

206

Tonolini and Di Pietro. Diffusion-weighted MRI of oedematous AP

5. Sheu Y, Furlan A, Almusa O, et al. The revised Atlanta classification for acute pancreatitis: a CT imaging guide for radiologists. Emerg Radiol 2012;19:237-43.
6. Zaheer A, Singh VK, Qureshi RO, et al. The revised Atlanta classification for acute pancreatitis: updates in imaging terminology and guidelines. Abdom Imaging 2013;38:125-36.
7. Foster BR, Jensen KK, Bakis G, et al. Revised Atlanta Classification for Acute Pancreatitis: A Pictorial Essay. Radiographics 2016;36:675-87.
8. Balthazar EJ, Robinson DL, Megibow AJ, et al. Acute pancreatitis: value of CT in establishing prognosis. Radiology 1990;174:331-6.
9. Ball CG, Correa-Gallego C, Howard TJ, et al. Radiation dose from computed tomography in patients with necrotizing pancreatitis: how much is too much ? J Gastrointest Surg 2010;14:1529-35.
10. Morgan DE, Ragheb CM, Lockhart ME, et al. Acute Pancreatitis: Computed Tomography Utilization and Radiation Exposure Are Related to Severity but Not Patient Age. Clin Gastroenterol Hepatol 2010;8:303-8.
11. Tonolini M, Valconi E, Vanzulli A, et al. Radiation overexposure from repeated CT scans in young adults with acute abdominal pain. Emerg Radiol 2018;25:21-7.
12. Miller FH, Keppke AL, Dalal K, et al. MRI of pancreatitis and its complications: part 1, acute pancreatitis. AJR Am J Roentgenol 2004;183:1637-44.
13. Shinya S, Sasaki T, Nakagawa Y, et al. The efficacy of diffusion-weighted imaging for the detection and evaluation of acute pancreatitis. Hepatogastroenterology 2009;56:1407-10.
14. Barral M, Taouli B, Guiu B, et al. Diffusion-weighted MR Imaging of the Pancreas: Current Status and Recommendations. Radiology 2015;274:45-63.
15. Qayyum A. Diffusion-weighted imaging in the abdomen and pelvis: concepts and applications. Radiographics 2009;29:1797-810.
16. Lee NK, Kim S, Kim DU, et al. Diffusion-weighted magnetic resonance imaging for non-neoplastic conditions in the hepatobiliary and pancreatic regions: pearls and potential pitfalls in imaging interpretation. Abdom Imaging 2015;40:643-62.
17. Shinya S, Sasaki T, Nakagawa Y, et al. Acute pancreatitis successfully diagnosed by diffusion-weighted imaging: a case report. World J Gastroenterol 2008;14:5478-80.
18. Thomas S, Kayhan A, Lakadamyali H, et al. Diffusion MRI of acute pancreatitis and comparison with normal individuals using ADC values. Emerg Radiol 2012;19:5-9.
19. Yencilek E, Telli S, Tekesin K, et al. The efficacy of diffusion weighted imaging for detection of acute pancreatitis and comparison of subgroups according to Balthazar classification. Turk J Gastroenterol 2014;25:553-7.
20. Hocaoglu E, Aksoy S, Akarsu C, et al. Evaluation of diffusion-weighted MR imaging in the diagnosis of mild acute pancreatitis. Clin Imaging 2015;39:463-7.
21. de Freitas Tertulino F, Schraibman V, Ardengh JC, et al. Diffusion-weighted magnetic resonance imaging indicates the severity of acute pancreatitis. Abdom Imaging 2015;40:265-71.
22. Wiggermann P, Grutzmann R, Weissenbock A, et al. Apparent diffusion coefficient measurements of the pancreas, pancreas carcinoma, and mass-forming focal pancreatitis. Acta Radiol 2012;53:135-9.
23. Momtahen AJ, Balci NC, Alkaade S, et al. Focal pancreatitis mimicking pancreatic mass: magnetic resonance imaging (MRI)/magnetic resonance cholangiopancreatography (MRCP) findings including diffusion-weighted MRI. Acta Radiol 2008;49:490-7.